Journal of Applied Polymer Science

Thermal stability, flame retardance, and mechanical properties of polyamide 66 modified by a nitrogen–phosphorous reacting flame retardant

Wenyan Lyu,[1] Yihua Cui,[1] Xujie Zhang,[1] Jingyao Yuan,[2] Wei Zhang[2]

[1]College of Materials Science and Technology, Nanjing University of Aeronautics and Astronautics, 29 Yudao Street, Nanjing 210016, China

[2]Nanjing Lihan Chemical Company, Limited, 1 Meilin Street, Nanjing 211102, China

Correspondence to: Y. H. Cui (E-mail: cuiyh@nuaa.edu.cn)

ABSTRACT: Flame-retardant polyamide 66 (PA66) was prepared by the polymerization between PA66 prepolymer and *N*-benzoic acid (ethyl-*N*-benzoic acid formamide) phosphamide (NENP). Compared with the pure PA66, the flame-retardant PA66 exhibited better thermal stability, as indicated by thermogravimetric analysis results. The limiting oxygen index was 28% and the UL-94 test results of the flame-retardant PA66 indicated a V-0 rating when the content of the NENP prepolymer was 5 wt %. The flammability and flame-retardant mechanism of PA66 were also studied with cone calorimetry and scanning electron microscopy/energy-dispersive X-ray spectroscopy, respectively. The mechanical properties results show that the flame-retardant PA66 resin had favorable mechanical properties. © 2016 Wiley Periodicals, Inc. J. Appl. Polym. Sci. **2016**, *133*, 43538.

KEYWORDS: flame retardance; mechanical properties; polyamides; thermal properties

Received 30 October 2015; accepted 12 February 2016

DOI: 10.1002/app.43538

INTRODUCTION

Polyamide 66 (PA66) contains a mixture of amine and acid group chains or a combination of two at their ends. It is a versatile engineering plastic and is characterized by its excellent mechanical properties and good processability.[1] Therefore, it is widely used in engineering applications because of its polar and polymorphic structure.[2] However, the application of PA66 is limited seriously because of the flammability of virgin PA66. To improve the flame retardancy of PA66, PA66 composites with added melamine cyanurate, red phosphorous, and clay as flame retardants were reported by Gijsman *et al.*,[3] Jou *et al.*,[4] and Rathi *et al.*,[5] respectively.

In recent years, intumescent flame retardants (IFRs) have been widely used in flammable polymers.[6] Compared to conventional flame retardants, several satisfactory advantages of IFRs include their high efficiency, halogen-free composition, and environmentally friendly characteristics.[7] Most studies have reported that IFRs are a mixture of three components, namely, an acid source, a carbon source, and a blowing agent. The acid source, usually essentially composed of poly(phosphoric acid), is promoted to form an impermeable char layer in the process of heating.[8] The carbon source is dehydrated by the acid, which is released from the acid source, and forms a semisolid and insulating carbonaceous layer on the surface of the polymer.[9] The blowing agent expands to form a multicellular char through the release of nonflammable gases.[10]

However, conventional IFRs still have some disadvantages.[11,12] For instance, to achieve a high flame-retarding level, a certain load of additive is necessary at the expense of the mechanical properties of the flame-retardant material; in particular, the impact strength decreases observably. Moreover, commonly used flame-retardant systems, which hardly withstand temperatures in excess of 200 °C through process of heating, cannot be incorporated into engineering plastics. To improve the thermal stability of flame retardants, several novel IFRs, which combined the acid source, carbon source, and blowing agents together to form a complex compound, have been prepared in recent decades.[13] The flame-retardant mechanism of the IFRs was different from those of traditional IFRs because of their more complicated structures, and a better thermal stability was obtained because of the higher molecular weight of the IFRs.[14]

As mentioned previously, with the P—N IFR system and the reaction characteristics of the PA66 propolymer, *N*-benzoic acid-(ethyl-*N*-benzoic acid formamide) phosphamide (NENP) was purchased from Nanjing LiHan Chemical Co, Ltd., because of its special P—N structures and dual —COOH groups.

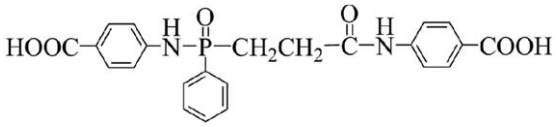

Figure 1. Structure of NENP.

The NENP structure is given in Figure 1. It was clear that NENP contained benzene and P and N elements, which could work as the carbon source, acid source, and gas source, respectively, and the NENP prepolymer, which could polymerize with the PA66 prepolymer, which was obtained through the reaction between adipic acid and hexamethylene diamine. Thus, to improve the flame retardancy of PA66, it was modified with NENP in this study. Moreover, the thermal stability, flame retardancy, and mechanical properties of PA66 with NENP were also studied.

EXPERIMENTAL

Materials

All of the starting materials were commercially available and were used without further purification. Industrial-pure-grade PA66 prepolymer was provided by BASF Co, Ltd. Chemically pure grade NENP was obtained from Nanjing LiHan Chemical Co, Ltd. Analytical-reagent-grade acetic acid and hexamethylene diamine were purchased from Shanghai Reagent Chemical Co, Ltd.

Polymerization of the Flame-Retardant PA66

Hexamethylene diamine (11.60 g, 0.10 mol) dissolved in ethyl alcohol (200 mL) was added to a glass flask; this was followed by the addition of NENP (39.60 g, 0.10 mol) to the mixture. The reaction mixture was stirred at 200 rpm and carefully heated gradually to 60 °C for hours. The NENP prepolymer was obtained by separation under reduced-pressure suction filtration and drying in a vacuum oven at 100 °C for 12 h. The synthetic route is shown in Scheme 1.

Then, the NENP prepolymer was used to replace equivalent amounts of PA66 prepolymer (0, 1, 3, and 5 wt %); these samples were defined as B1, B2, B3, and B4, respectively. The polymerization reaction of the flame-retardant PA66 was performed at 1.7 MPa and 280 °C.

Preparation of the Test Sample

Before melt injection, the flame-retardant PA66 particles were dried at 100 °C for 24 h. The PA66 pellets were molded into a standard sample (80 × 10 × 4 mm^3) for limiting oxygen index (LOI) characterization, rectangular bars (100 × 7.1 × 3.2 mm^3) for the UL-94 vertical burning test, a standard sample (120 × 10 × 4 mm^3) for tensile testing, and rectangular bars (80 × 10 × 4 mm^3) for notched Izod impact testing with a HTF80X1 injection-molding machine from Haitian Plastic Machinery, Ltd., in the temperature range 250–265 °C.

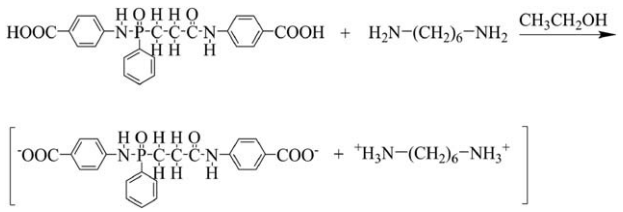

Scheme 1. Synthetic route of the NENP prepolymer.

Table I. Formulations and Physical Constants of the PA66 Resin

Sample	NENP prepolymer (g)	PA66 prepolymer (g)	η (dL/g)	Melt flow index (g/10 min)
B1	0	1000	106.1	40
B2	10	990	105.9	42
B3	30	970	105.1	44
B4	50	950	104.7	47

Thermogravimetric analysis (TGA) and differential scanning calorimetry (DSC) were performed with a Pyris 1 thermal analyzer (PerkinElmer). The powder sample prepared through grinding (2.5 mg for TGA, 8.0 mg for DSC) was placed inside an Al_2O_3 crucible, and the measurement was carried out in the range 25–600 °C at a heating rate of 10 °C/min under a nitrogen atmosphere. The initial degradation temperature of the flame-retardant PA66 was evaluated by the temperature at 5 wt % weight loss (T_5), the temperature at 50 wt % weight loss (T_{50}), and the peak temperature of the maximum weight loss (T_p).

RESULTS AND DISCUSSION

Analysis of the Physical Constant

Detailed formulations and physical constants of the sPA66 resin are listed in Table I. The intrinsic viscosity (η) and melt flow index were tested by the capillary tube method and a melt flow instrument, respectively. η decreased and the melt flow index increased with increasing content of NENP prepolymer because the movement of the PA66 main chain was restricted by benzene rings with a large steric hindrance; this diminished chain involvement.

Thermal Stability of the PA66 Resin

The TGA curves of the PA66 resin in a nitrogen environment are shown in Figure 2. In nitrogen ambient atmospheres, the

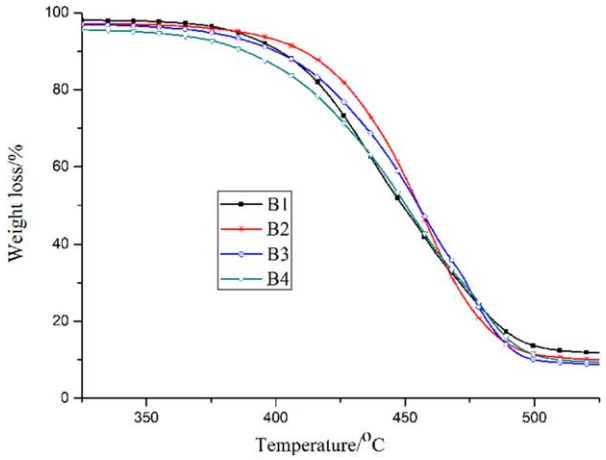

Figure 2. TGA curves of the PA66 resin. [Color figure can be viewed in the online issue, which is available at wileyonlinelibrary.com.]

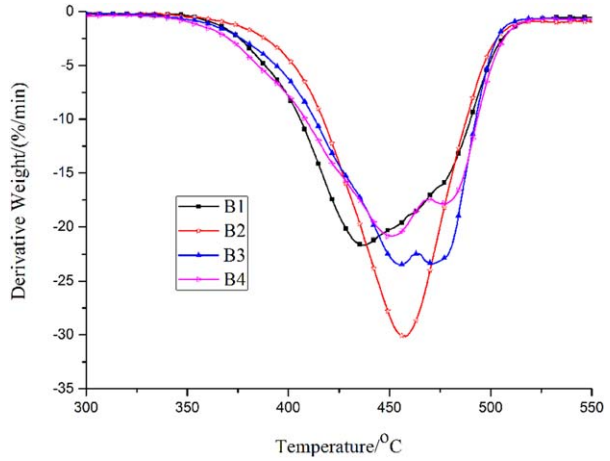

Figure 3. Derivative thermogravimetry curves of the PA66 resin. [Color figure can be viewed in the online issue, which is available at wileyonlinelibrary.com.]

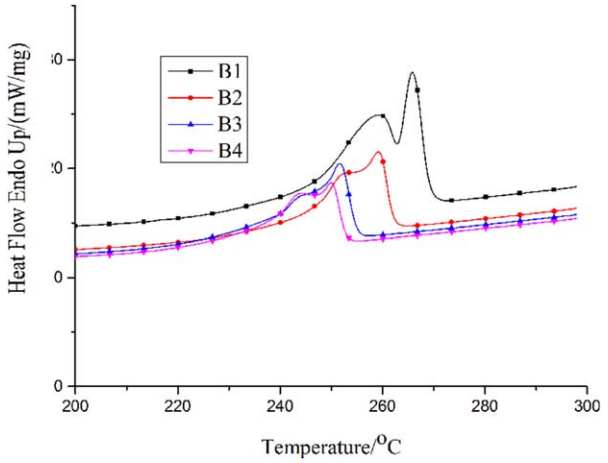

Figure 4. DSC curves of the PA66 resin (heating). [Color figure can be viewed in the online issue, which is available at wileyonlinelibrary.com.]

initial decomposition temperature (T_5) of the flame-retardant PA66 (347 °C) was 38 °C lower than that of pure PA66 (385 °C) when the content of NENP prepolymer was 5 wt %, but the weight loss peak temperature (T_{p1}) increased 19 °C from 437 to 456 °C (Figure 3). It was clear that the rate of weight loss decreased with increasing temperature. Otherwise, the rate of flame-retardant PA66 slowed down to a certain degree when PA66 was modified by NENP. Therefore, the mass loss rate was reduced remarkably. The thermal behavior of the PA66 in the nitrogen atmosphere indicated that the addition of NENP improved the thermal stability of PA66, although the initial decomposition temperature decreased. The volatilization rate of the flame-retardant PA66 was faster than that of the pure PA66 at the beginning; thereafter, the weight loss decreased compared to that of the pure PA66, probably because NENP contained three benzene rings, which had better heat resistance than CH_2 chains, and a conjugated system with a strong electron-withdrawing ability in the process of thermal decomposition was formed by three benzenes ring around the P═O group, and thus, more heat had to be absorbed to disorder this stable system.[15] At the same time, the PO· free radicals released from the aryl phosphine oxide could promote the crosslinking degree of PA66 in the process of thermal decomposition. Therefore, the heat-resistant properties of the PA66 chain segments improved.[16] The details of TGA are listed in Table II. It was interesting that there were two T_ps in samples B3 and B4; this may have been due to small molecules of flame retardant produced in the thermal decomposition process; these promoted pieces of PA66 to crosslink. Thus, the thermal stability of PA66 was improved by the higher heat-resistant chain segment.

Table II. TGA Results for the PA66 and Flame Retardancy of PA66

Sample	T_5 (°C)	T_{50} (°C)	T_{p1} (°C)	T_{p2} (°C)
B1	385	449	437	—
B2	384	455	458	—
B3	373	455	455	470
B4	347	455	456	480

T_{p2} is defined as the second weight loss temperature.

The DSC curves of PA66 resin in the nitrogen environment are shown in Figures 4 and 5. The percentage crystallinity of the PA66 samples was calculated as the ratio of the heat of fusion (ΔH_m) of the sample to the ΔH_m of the pure crystalline form of PA66, which was taken as 195.00 J/g. Table III lists the DSC details of the PA66 resin. It was clear that the melting temperature (T_m), glass-transition temperature (T_g), and crystallinity decreased continuously with the further addition of NENP. This was probably because the barrier effect of rigid benzene rings in the NENP chains obviously limited the movement of the PA66 chains; this decreased the rate of crystallization of the PA66 matrix.[17]

Flame-Retardant Properties of PA66

The results of LOI and UL94 tests at a 3.2-mm thickness of PA66 are listed in Table IV. The UL-94 rating and LOI value were higher when the NENP content was relatively higher. A V-0 rating was achieved when the content of the NENP

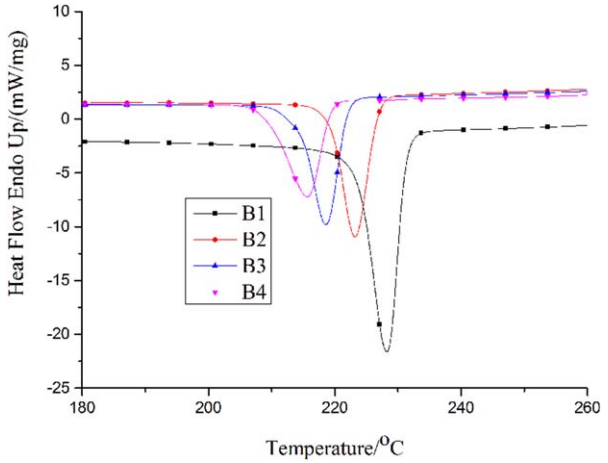

Figure 5. DSC curves of the PA66 resin (cooling). [Color figure can be viewed in the online issue, which is available at wileyonlinelibrary.com.]

Table III. DSC Results for the PA66 and Flame Retardancy of PA66

Sample	T_m (°C)	ΔH_m (J/g)	T_g (°C)	X_c
B1	265.78	−59.60	231.31	30.56
B2	259.26	−57.56	227.00	29.52
B3	251.63	−55.27	222.23	28.34
B4	249.99	−50.31	219.61	25.80

X_c is defined as the degree of crystallinity of PA66.

Table IV. Flame Retardancy Properties of the PA66 Resin

Sample	LOI	UL-94 3.2-mm rating	Cotton indicator ignited by melt drips	Self-extinguish time (s)
B1	23	V-2	Yes	6
B2	25	V-2	Yes	8
B3	26	V-1	No	11
B4	28	V-0	No drips	7

prepolymer was 5 wt %. The previous experimental phenomena could be explained by the fact that NENP promoted the formation of nitrogen-containing nonflammable gases and, thus, blocked the transfer of combustion improver and flammable gas and effectively shortened the afterflame time. Moreover, the phosphorus element in NENP could make up for the lack of the condensed-phase composition. Therefore, the increase in the NENP content increased the melt viscosity and decreased the dropping rate. This effectively blocked the transfer of the interior heat of the melt drips to the surface and reduced the flammability of the melt drips.[18] In addition, the extinguishing times of the flame-retardant PA66 were longer than that of pure PA66. This was because the flame was carried off with melt drip in the combustion process of pure PA66; however, the char-forming characteristic of the flame-retardant PA66 was improved by the addition of NENP and induced the char layer to cover the surface of PA66 and overcome the drip. Thus, the extinguishing time of the flame-retardant PA66 was delayed.

The LOI of PA66 is shown in Table IV. A moderate NENP prepolymer content (5 wt %) improved the highest LOI value. This also showed N—P synergistic effects between P and N elements in the main chain of the flame-retardant PA66. In general, N—P synergistic action was explained by the interaction between P and N flame retardants and produced macromolecular substances with a higher thermal stability to further consolidate the condensed phase.[19] The test samples are shown in Figure 6.

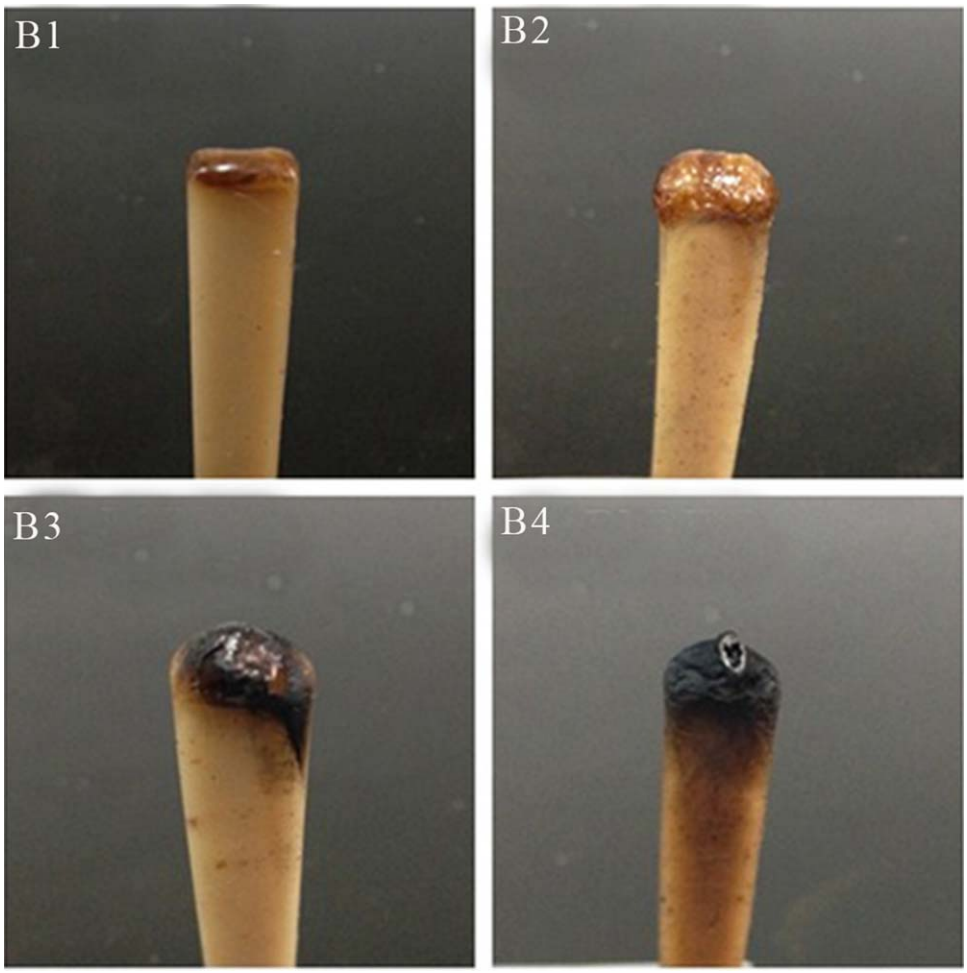

Figure 6. Flammability test samples of the PA66 resin. [Color figure can be viewed in the online issue, which is available at wileyonlinelibrary.com.]

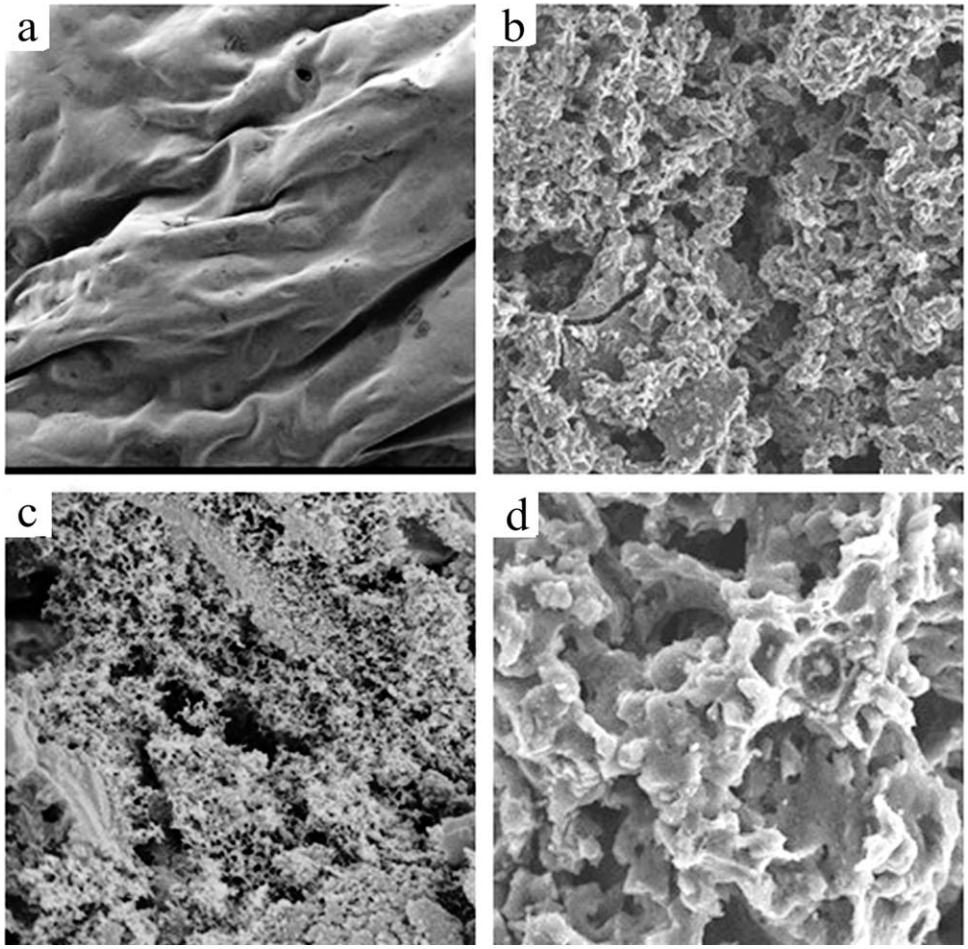

Figure 7. Micromorphology of the char layer.

Microstructure of Char Layer Analysis

To elucidate the mechanism of flame retardance on the formation of an intumescent char layer, the microstructure of char residue after carbonization was investigated by scanning electron microscopy (SEM)/energy-dispersive X-ray spectroscopy (EDX).

Figure 7 shows the char layer micromorphology of the flame-retardant PA66. The relatively smooth, uniform, and compact stack layer with a significant amount of char was found in the sample generated from combustion; this indicated that a strong char layer was formed, and it transferred heat. Also, the penetration of oxygen and combustible gases was effectively prevented. In the meantime, some microholes were observed on the surface of the char layer because nonflammable NH_3 and H_2O gases were produced from the crack of the P—N bond during the thermal decomposition process. NH_3 and H_2O diffused to the surface through random channels and formed a protective gas layer; this diluted the material thermal decomposition of the combustible gas and cut off oxygen to the inside of material. This delayed the spread of the burning flame, if one assumes that the nitrogen elements functioned as the blowing agent and isolated the transfer of combustible gases to the inner part of the material; it thus played a very important role in the flame-retardance process.[20]

To illustrate the contribution of phosphorus to the formation of carbonized layer, EDX images were obtained from the area scan result by SEM. Figure 8 shows that the char layer mainly contained C [Figure 8(b)], O [Figure 8(c)], and P [Figure 8(d)]; this indicated that phosphorus elements in NENP played an important role in the thermal decomposition process. The crosslinking reaction between PA66 and PO· produced by the thermal decomposition of phosphorus compounds led to the formation of a three-dimensional structure. Moreover, PO· promoted the dehydration of small molecules decomposed from PA66 to form a density layer, which covered the surface of PA66 and prevented the exchange of oxygen and heat.[21]

Cone Calorimetry

Cone calorimetry is considered one of the most important parameters for evaluating the flame retardancy of a polymer. Figures 9–11 show the heat release rate (HRR), total heat release (THR), and total smoke produce (TSP) curves of the PA66 resin, respectively; this indicated that the addition of NENP resulted in the sharp peaks, which tended to decrease in a manner similar to the other polyamide flame-retardancy composites.[22] The THR and TSP decreased markedly with increasing NENP content. The results of HRR, THR, and TSP confirmed that NENP was affected through the gas-phase flame-retardancy mechanism. The details of cone calorimetry are listed in Table V.

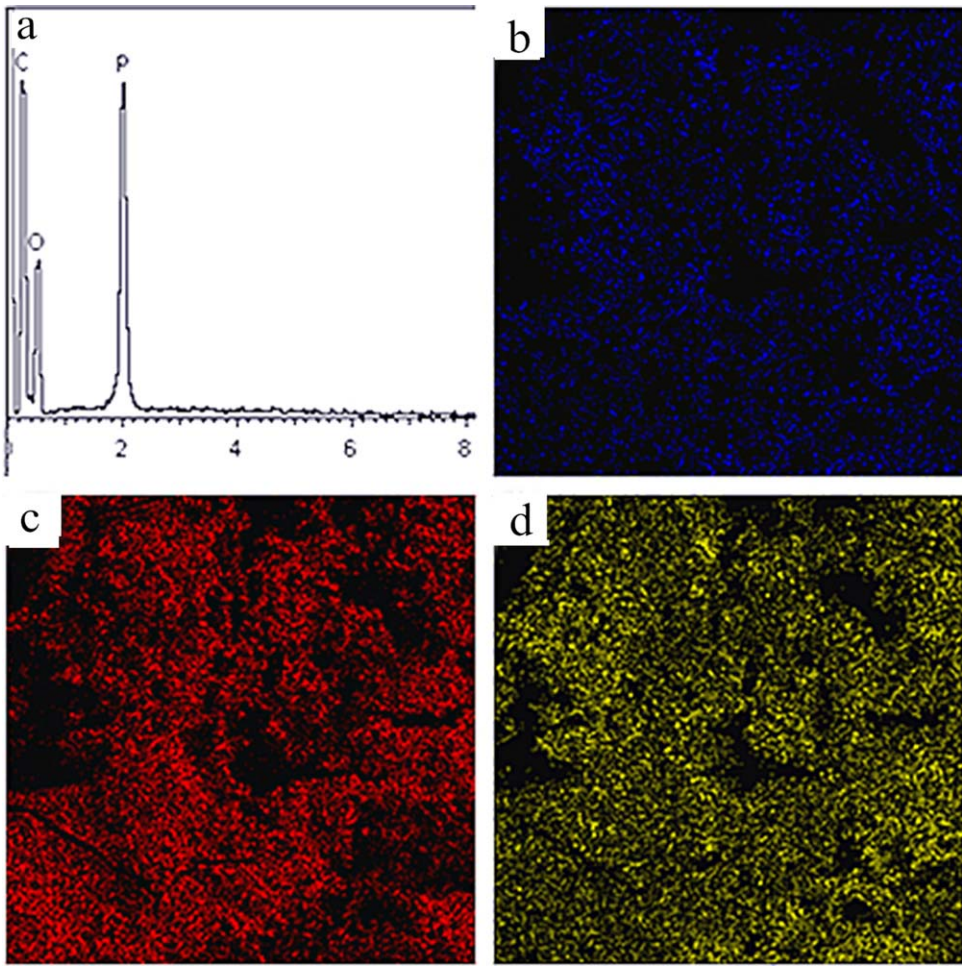

Figure 8. Elemental distribution of the char layer. [Color figure can be viewed in the online issue, which is available at wileyonlinelibrary.com.]

Previous studies have suggested that the lower flammability of a polymer with a phosphorus-containing flame retardant is due to the formation of PO· free groups and a multilayer carbonaceous structure. During combustion, NENP released NH_3 and PO· and degraded to form phosphoric acid derivative. The release of NH_3 and PO· in the PA66 matrix induced the cross-linking reaction of the PA66 matrix and created a physical protective barrier on the surface of PA66; this was produced from the reaction between the phosphoric acid derivative, and the decomposition products of PA66 may have insulated the underlying polymeric substrate from the heat source and slowed down heat and mass transfer.[23]

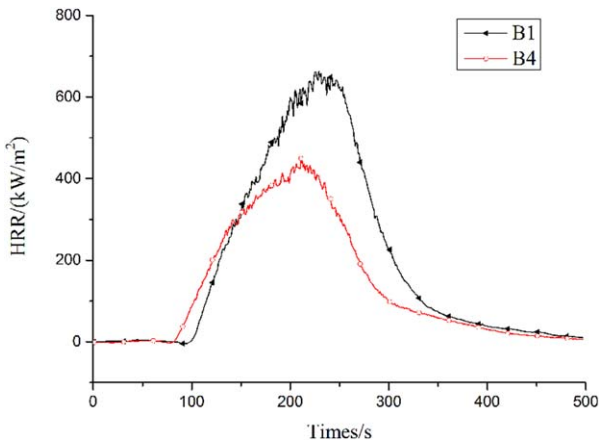

Figure 9. HRR curves of the PA66 resin. [Color figure can be viewed in the online issue, which is available at wileyonlinelibrary.com.]

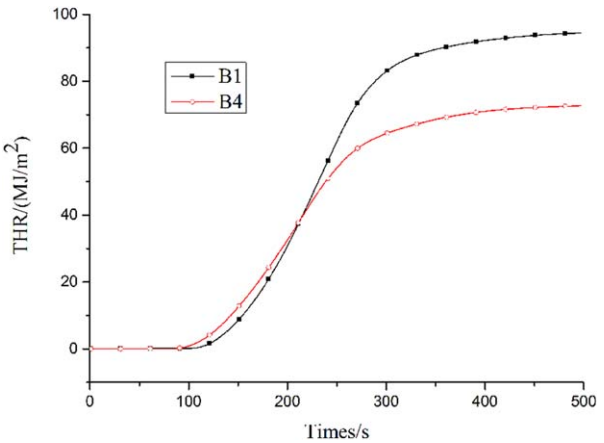

Figure 10. THR curves of the PA66 resin. [Color figure can be viewed in the online issue, which is available at wileyonlinelibrary.com.]

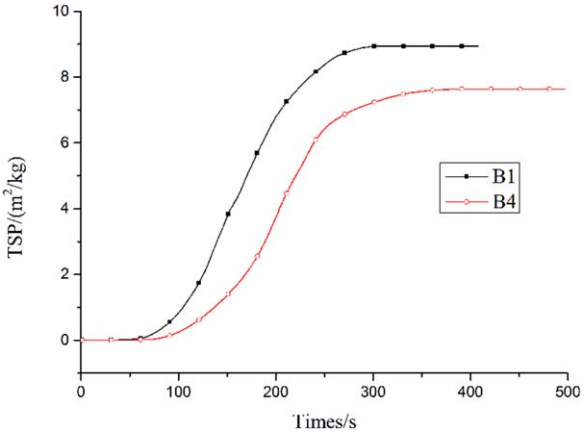

Figure 11. TSP curves of the PA66 resin. [Color figure can be viewed in the online issue, which is available at wileyonlinelibrary.com.]

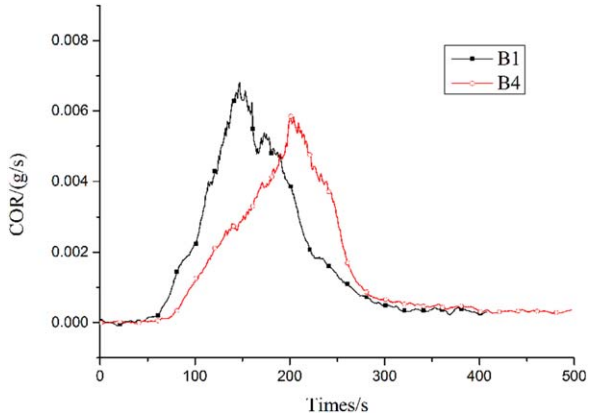

Figure 12. COR curves of the PA66 resin. [Color figure can be viewed in the online issue, which is available at wileyonlinelibrary.com.]

The harmful toxic gases of the combustion process to the human body mainly include CO, NO, and HCN. Therefore, the analysis of the polymer combustion toxicity is of significant importance. Figure 12 shows the CO release rate (COR) of the flame-retardant PA66 resin. As shown by Figure 12 and Table V, when the NENP content increased up to 5 wt %, the COR of flame-retardant PA66 obviously decreased; this indicated that the toxic gas emission from the burning of PA66 decreased, and this decreased harmful effects to the human body.

Mechanical Properties of PA66

Figures 13 and 14 show the bending strength and bending modulus, tensile strength, and notch impact strength of flame-retardant PA66, respectively; this indicated that the tensile strength, bending strength, and bending modulus decreased slightly with increasing NENP content, but the notched impact strength increased relatively. Combined with the DSC results, the change in the mechanical properties was closely related to the crystallization performance of PA66. The crystallization properties of PA66 were affected by the structure of rigid benzene groups in the process of cooling polymerization. Because of the apparent space steric hindrance and crystallization inhibition effect, the benzene ring in NENP decrease the crystallinity of PA66 in the process of crystallization.[24] Moreover, with further increases in the NENP content, the space effect was more and more obvious.

The NENP flame-retardant PA66 overcame the significantly decreasing impact strength of the substrate material, which was modified by the addition of traditional flame retardant, while maintaining the excellent tensile strength, bending strength, and bending modulus.[25] When the NENP prepolymer content reached 5 wt %, the tensile strength, bending strength, and

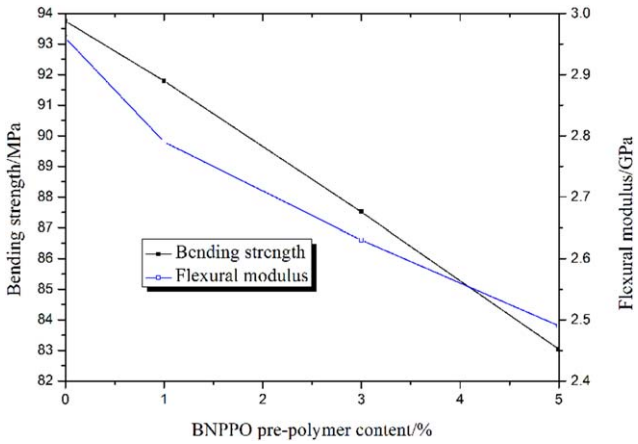

Figure 13. Bending strength and modulus curves of the PA66 resin. [Color figure can be viewed in the online issue, which is available at wileyonlinelibrary.com.]

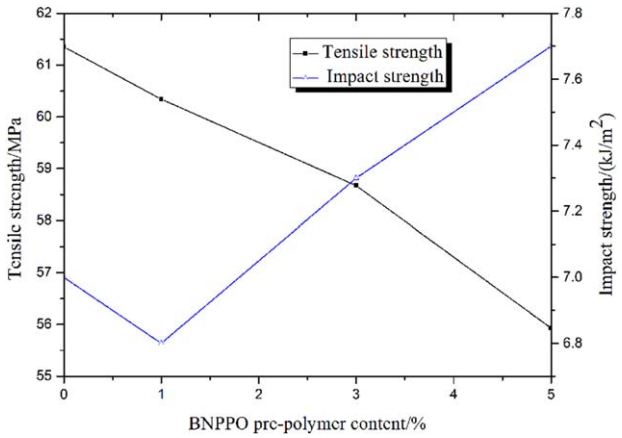

Figure 14. Tensile and impact strength of the PA66 resin. [Color figure can be viewed in the online issue, which is available at wileyonlinelibrary.com.]

Table V. Data Details for the Cone Calorimeter

Sample	HRR (kW/m²)	THR (MJ/m²)	TSP (m²/kg)	COR (g/s)
B1	648.47	94.46	8.94	6.81×10^{-3}
B4	432.57	72.86	7.63	5.83×10^{-3}

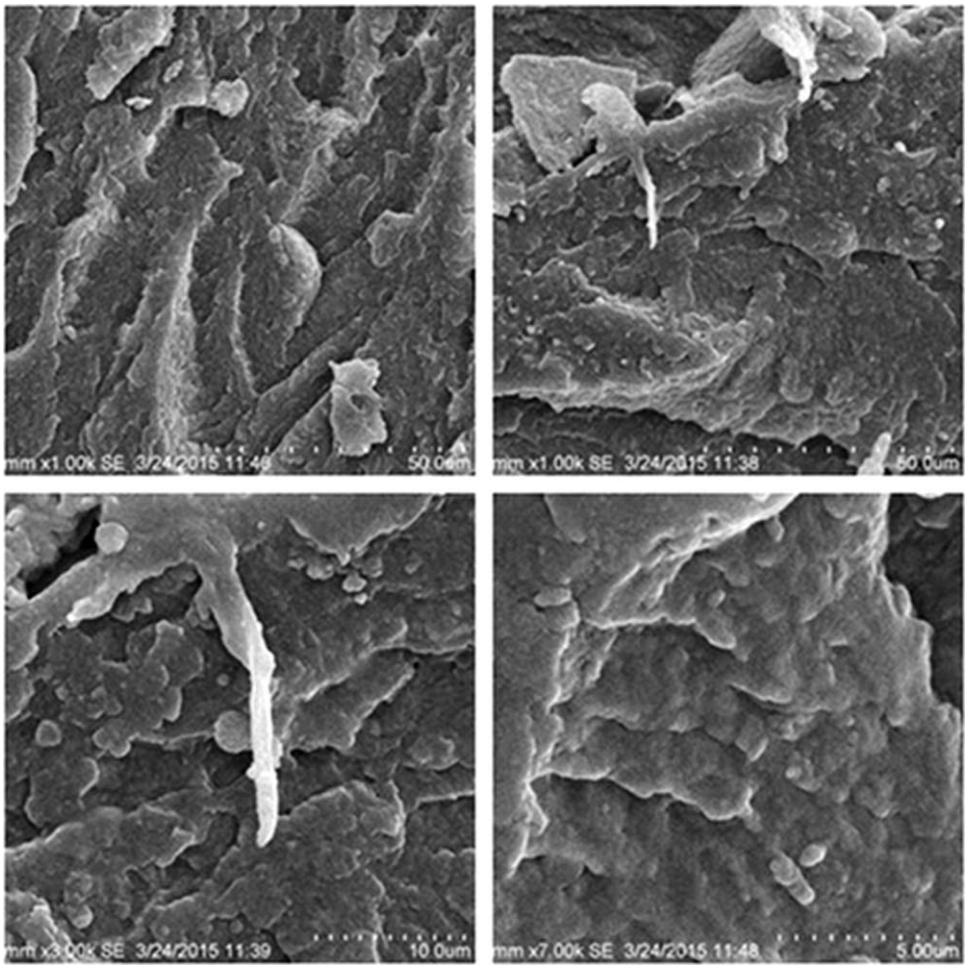

Figure 15. Micromorphology of the impact sample.

bending modulus of the flame-retardant PA66 were 55.93 MPa, 83.04 MPa, and 2.49 GPa; these were decreases of 8.83, 11.42, and 8.83% compared to those of pure PA66, respectively. However, the impact strength was 0.7 kJ/m^2 higher than that of pure PA66; it went from 7.0 to 7.7 kJ/m^2.

Microstructure of the Notched Impact Sample

To study the fracture mechanism of the flame-retardant PA66 modified by NENP and illustrate the effects of NENP on the mechanical properties of the flame-retardant PA66, the impact fracture microstructure of PA66 modified by 5 wt % NENP per polymer was studied by SEM. The SEM images shown in Figure 15 clearly indicate that the flame-retardant PA66 had ductile fracture. The section cracks showed inhomogeneous tearing crack characteristics; this indicated a large number of burr and obvious interlayer sliding phenomena.[26]

CONCLUSIONS

At a 5 wt % content of NENP prepolymer, T_5 of the flame-retardant PA66 was 38 °C lower than that of pure PA66, but the T_p increased 19 °C from 437 to 456 °C, indicating that the flame-retardant PA66 with NENP keeps a better thermal stability.

For PA66 with 5 wt % NENP prepolymer, the UL-94 test indicated a V-0 rating and the LOI value was 28%; this indicated that PA66 modified by NENP had outstanding flame-retardant properties.

The tensile strength, bending strength, bending modulus, and notched impact strength of PA66 reached 55.93 MPa, 83.04 MPa, 2.49 GPa, and 7.7 kJ/m^2, respectively, when the content of NENP prepolymer was 5 wt %. These results illustrate that the NENP flame-retardant PA66 maintained well-deserved mechanical properties.

ACKNOWLEDGMENTS

This work was supported by Nanjing Lihan Chemical Co., Ltd., and the Key Science and Technology Supporting Projects of Jiangsu Province (BE2013012-3), and it was funded by the Priority Academic Program Development of Jiangsu Higher Education Institution.

REFERENCES

1. Dasari, A.; Yu, Z. Z.; Yang, M. S.; Zhang, Q. X.; Xie, X. L.; Mai, Y. W. *Compos. Sci. Technol.* **2006**, *66*, 3097.
2. Shen, L.; Phang, I. Y.; Chen, L.; Liu, T. X.; Zeng, K. Y. *Polymer* **2004**, *45*, 3341.
3. Gijsman, P.; Steenbakkers, R.; Fürst, C.; Kersjes, J. *Polym. Degrad. Stab.* **2002**, *78*, 219.

4. Jou, W. S.; Chen, K. N.; Chao, D. Y.; Lin, C. Y.; Yeh, J. T. *Polym. Degrad. Stab.* **2001**, *74*, 239.
5. Dahiya, J. B.; Rathi, S.; Bockhorn, H.; Haußmann, M.; Kandola, B. K. *Polym. Degrad. Stab.* **2012**, *97*, 1458.
6. Enescu, D.; Frache, A.; Lavaselli, M.; Monticelli, O.; Marino, F. *Polym. Degrad. Stab.* **2013**, *98*, 297.
7. Zhan, J.; Song, L.; Nie, S. B.; Hu, Y. *Polym. Degrad. Stab.* **2009**, *94*, 291.
8. Chen, X. L.; Jiao, C. M. *Fire Saf. J.* **2009**, *44*, 1010.
9. Gao, F.; Tong, L. F.; Fang, Z. P. *Polym. Degrad. Stab.* **2006**, *91*, 1295.
10. Ma, H. Y.; Tong, L. F.; Xu, Z. B.; Fang, Z. P.; Jin, Y. M.; Lu, F. Z. *Polym. Degrad. Stab.* **2007**, *92*, 720.
11. Ma, H. Y.; Fang, Z. P. *Thermochim. Acta* **2012**, *543*, 130.
12. Alongi, J.; Poskovic, M.; Visakh, P. M.; Frache, A.; Malucelli, G. *Carbohydr. Polym.* **2012**, *88*, 1387.
13. Pinto, U. A.; Léa, L.; Visconte, Y.; Célia, R.; Nunes, R. *Polym. Degrad. Stab.* **2000**, *69*, 257.
14. Yang, K.; Xu, M. J.; Li, B. *Polym. Degrad. Stab.* **2013**, *98*, 1397.
15. Sharma, S.; Harper, M. R.; Green, W. H. *Combust. Flame* **2010**, *157*, 1331.
16. Ren, H.; Sun, J. Z.; Wu, B. J.; Zhou, Q. Y. *Polym. Degrad. Stab.* **2007**, *92*, 956.
17. Shabbir, S.; Zulfiqar, S.; Ahmad, Z.; Sarwar, M. I. *Polym. Degrad. Stab.* **2010**, *95*, 1251.
18. Levchik, S. V.; Weil, E. D.; Lewin, M. *Polym. Int.* **1999**, *48*, 532.
19. Liu, Y.; Wang, Q. *Polym. Degrad. Stab.* **2006**, *91*, 3103.
20. Naik, A. D.; Fontaine, G.; Samyn, F.; Delva, X.; Bourgeois, Y.; Bourbigot, S. *Polym. Degrad. Stab.* **2013**, *98*, 2653.
21. Yang, H. Y.; Song, L.; Tai, Q. L.; Wang, X.; Yu, B.; Yuan, Y.; Hu, Y.; Yuen, R. K. K. *Polym. Degrad. Stab.* **2014**, *105*, 248.
22. Buczko, A.; Stelzig, T.; Bommer, L.; Rentsch, D.; Heneczkowski, M.; Gaan, S. *Polym. Degrad. Stab.* **2014**, *107*, 158.
23. Braun, U.; Schartel, B.; Fichera, M. A.; Jäger, C. *Polym. Degrad. Stab.* **2007**, *92*, 1528.
24. Yan, X. L.; Imai, Y.; Shimamoto, D.; Hotta, Y. *Polymer* **2014**, *55*, 6186.
25. Yang, X. F.; Li, Q. L.; Chen, Z. P.; Han, H. L.; Jing, H. X. *J. Compos. Mater.* **2009**, *43*, 2785.
26. Zhang, X.; Li, Y. B.; Zuo, Y.; Lv, G. Y.; Mu, Y. H.; Li, H. *Compos. A* **2007**, *38*, 843.